RESEARCH ARTICLE

Silicon improves root system and canopy physiology in wheat under drought stress

**Waseem Ashfaq · Graham Brodie ·
Sigfredo Fuentes · Alexis Pang · Dorin Gupta**

Abstract

Aims Root system is an important regulator for unevenly distributed below-ground resource acquisition. In a rainfed cropping environment, drought stress (DS) significantly restricts root growth and moisture uptake capacity. The fact that silicon (Si) alleviates DS in wheat is widely reported, but its effects on the wheat root system remain unclear.

Methods The present study investigated the effect of pre-sowing Si treatment on two contrasting wheat cultivars (RAC875, drought-tolerant; Kukri, drought-susceptible) at early growth stages. The cultivars were grown in a glasshouse in a complete randomized design with four replications and two watering treatments. Various root traits and physiological data, including non-destructive infrared thermal imaging for water stress indices, were recorded.

Results Under DS and Si (DSSi), Kukri had a significant increase in primary root length (PRL, 44%) and lateral root length (LRL, 28.1%) compared

with RAC875 having a substantial increase in PRL (35.2%), but non-significant in LRL. The Si-induced improvement in the root system positively impacted canopy physiology and significantly enhanced photosynthesis, stomatal conductance and transpiration in Kukri and RAC875 under DSSi. Canopy temperature was reduced significantly in Kukri (4.24%) and RAC875 (6.15%) under DSSi, while canopy temperature depression was enhanced significantly in both the cultivars (Kukri, 78.6%; RAC875, 58.6%) under DSSi.

Conclusion These results showed that Si has the potential to influence below-ground traits, which regulate the moisture uptake ability of roots for cooler canopy and improved photosynthesis under DS. It also suggests a future direction to investigate the underlying mechanisms involved in wheat's Si-induced root growth and moisture uptake ability.

W. Ashfaq · S. Fuentes · A. Pang · D. Gupta (✉)
School of Agriculture, Food and Ecosystem Sciences, Faculty of Science, The University of Melbourne, Melbourne, Australia
e-mail: dorin.gupta@unimelb.edu.au

G. Brodie
College of Science and Engineering, James Cook University, Townsville, QLD, Australia

Introduction

Risks of crop failures to varying degrees are predicted to increase due to changing climate (chapter 5: IPCC 2019). Among all the climatic risks, drought (*substantial and sustained reduction in soil moisture availability*) is one of the main limiting

factors for crop growth and productivity and has been widely reported (Khadka et al. 2020). Drought stress significantly affects crop productivity by impairing various morpho-physiological processes and leading to significant yield losses on a global scale (Khadka et al. 2020; Raza et al. 2023). There are various approaches to enhance crop resilience to cope with drought stress, either through improved plant genetics, improved resource allocation and utilization within the canopy or through supplementation of nutrients to enhance plant growth of above and below-ground parts, specifically when plants are under stress. Historically, due to the practical difficulties in phenotyping the hidden half, the persistent genetic gains delivered by crop breeding programs have relied predominantly on manipulating above-ground plant features. This overlooks the root system improvement and has been subjected to unintentional indirect selection with higher grain yield in the targeted environment (Wasson et al. 2012; Bishopp and Lynch 2015).

The roots are fundamentally crucial for plants, making a root-soil interface for the nutrients and water uptake required for optimum growth (Ober et al. 2021). The roots are the first organ to sense soil drying and the subsequent origin of the chemical and hydraulic signals to modulate the plant morphology, phenology and physiology. Root characteristics are governed by plant genetics, intercropping patterns, planting density, edaphic conditions, seasonal weather and agronomic practices (Meister et al. 2014). Soil drying increases soil impedance, changes the soil texture, reduces the soil water holding capacity and limits sufficient root growth. To optimize soil resource acquisition, useful root functional traits must be identified, and their contribution to plant performance must be ascertained (York et al. 2013). Studies have shown that targeted selection for specific root system components could improve crop yield in dryland cropping systems. Evidence for these claims is taken from the findings of a well-validated crop simulation modelling study conducted in Australia that deeper and vertical patterns of wheat (*Triticum aestivum* L.) root systems could significantly improve nitrogen and moisture uptake (Lilley and Kirkegaard 2011). Root development is highly responsive to available edaphic factors and environmental needs where they grow. Even minor variations in the root's micro-environment can alter the

density, pattern and length of the lateral roots (Bao et al. 2014).

Wheat has a fibrous root system, and two types of roots are mainly prominent in root system architecture (RSA); (i) seminal or primary axile roots (PR), which develop from the embryonic hypocotyls of the germinal caryopsis; and (ii) adventitious or nodal axile roots, which subsequently emerge from the basal nodes of the apical culm and associated tillers. With the emergence of leaves and tillers, fine lateral roots (branches) develop from primary and nodal roots. The lateral roots are mainly responsible for nutrient and water uptake and provide high plasticity to the overall rooting system (Tang et al. 2011). Early root growth and proliferation are indispensable in below-ground resource acquisition (i.e., phosphorus, nitrogen and water) for early plant development (Waines and Ehdaie 2007). Root traits, i.e., higher root length density (deeper roots), reduced horizontal distribution near the topsoil and increased branching at depth (Wasson et al. 2012), root penetration to deeper layers and higher subsoil extraction (Lilley and Kirkegaard 2011), are considered essential for efficient soil-resource acquisition under drought stress. These RSA components are correlated with maintaining and facilitating plant productivity in the water-limited environment, along with improved above-ground plant traits contributing to drought tolerance.

Silicon (Si) application to alleviate abiotic stresses has become a promising prospect in recent decades. Although Si is the 2nd most abundant element in the geosphere after oxygen, it is not readily available to plants for uptake due to its polymerized form (Debona et al. 2017). The root epidermis absorbs Si in monosilicic acid form (H_4SiO_4) at <9 pH (Tubaña and Heckman 2015) and subsequently translocate it to the stem and leaves by the transpirational stream through the xylem (Debona et al. 2017). Although Si is considered a non-essential plant element, a large number of studies have shown that Si has beneficial effects on plant development and productivity, especially under stressful conditions, i.e., drought (Debona et al. 2017; Luyckx et al. 2017). All soil-grown plants may contain Si in their tissues ranging from 0.1–10% of their total dry matter (TDM), mainly attributed to varying Si uptake ability by the roots of different plant species (Debona et al. 2017). Based on the amount of biogenic Si found in tissues,

plant species are grouped into Si accumulator (accumulate Si up to 10% of their TDM, generally monocotyledonous families, i.e., Poaceae and Cyperaceae), intermediator (melon, cucumber, strawberry) and the excluder (tomato, beans, lentil, canola, potato; < 1% of their TDM) types (Liang et al. 2006; Souri et al. 2021).

The Si role in drought alleviation may be attributed to its facilitating role in the up-regulation of aquaporin proteins, increased root hydraulic conductivity (Liu et al. 2014; Wang et al. 2021), improved photosynthetic and antioxidant activities to minimize the damaging effect of reactive oxygen species in cells (Debona et al. 2017), maximize photosystem II (PSII) quantum efficiency (Luyckx et al. 2017) and improved osmotic adjustments through osmolytes and hydrolytic enzymes accumulation (Biju et al. 2017; Wang et al. 2021). Impairments in cell water balance, PSII efficiency and gaseous exchange apparatus are the primary mechanisms by which drought stress affects plant productivity. Silicon application has been proven to minimize the effects of these impairments (Debona et al. 2017; Luyckx et al. 2017). The improvements in Si-induced plant water use efficiency have been associated with increased silicification in the leaf epidermis to prevent water escape through leaf stomata (Debona et al. 2017). These growing evidence suggests that Si may influence various morpho-physiological traits associated with drought stress tolerance. However, further research is required to determine how Si potentiates drought alleviation mechanisms via roots and canopy traits for improved photosynthesis and other canopy related attributes under drought stress.

Therefore, given the beneficial role of Si under drought stress and the research gaps discussed above, the current study aimed (i) to identify and characterize phenotypic variability in the canopy-related traits and root systems of two wheat cultivars in response to pre-sowing Si treatment under drought stress, and (ii) to determine the relationship between roots and canopy physiology related traits, including computational water stress indices (canopy temperature depression (CTD, °C); canopy temperature (T_c, °C) crop water stress index (CWSI, adimensional); reference temperatures for stressed (T_{dry}, °C) and non-stressed crop (T_{wet}, °C) and stomatal conductance index, I_g), for optimum plant performance in a drought-stressed condition.

Material and methods

Plant material

Two contrasting bread wheat cultivars, RAC875 and Kukri, were used as experimental materials. RAC875, a wheat breeding line with excellent grain quality, had shown a relatively stable grain yield in the dry environment of South Australia (Izanloo et al. 2008). Kukri, a hard white wheat variety, endures significantly lower grain yield in moderate to lower rainfall regions (Bennett et al. 2012; Fleury et al. 2010). Both cultivars have similar phenology (3–5 days heading time difference) under normal growing conditions and possess Rht2 semi-dwarfing genes (Izanloo et al. 2008).

Experimental design and setup

Three factors factorial experiment (two wheat cultivars, two Si levels and two watering levels) was used to allocate the treatments in a complete randomized design with four replicates (one pot = one replication unit). Before sowing, Si was applied in two treatments ($Si_0 = 0$ mM or no Si and $Si_1 = 4$ mM, sodium metasilicate pentahydrate; $Na_2SiO_3.5H_2O$ was used to make 4 mM Si solution with adjusted pH = 7) and thoroughly mix into a standard potting mix (4:4:1:1 compost pine bark med (0-6 mm): compost pine bark coarse (5-12 mm): processed sawdust: river sand, pH ~ 6.0) using spray bottle (Alzahrani et al. 2018). Plants were grown in round-shaped perforated nursery pots (25 × 25 cm in height and depth) filled with the same mass of oven-dried potting mix. Six seeds were sown and later thinned to four plants per pot. Polylining was applied to the bottom of each pot to prevent the highly soluble Si from leaching.

To estimate the potting mix's field capacity, two perforated pots filled with oven-dried potting mix were saturated with tap water and allowed to drain for six hours. Following this, 250 g of the potting mix was sampled from the centre of each pot to record the wet mass. Samples were then oven-dried at 70 °C for 72 hours to determine the dry mass of sampled potting mix. The gravimetric water content (%) of the potting mix was

measured using equation-1 (Pepper and Brusseau 2019).

$$\text{Gravimetric water contents (\%)} = \frac{\text{Wet mass (gm)–Dry mass (gm)}}{\text{Dry mass (gm)}} \times 100 \tag{1}$$

Growth conditions

Plants were grown in a controlled-temperature glasshouse at The University of Melbourne, Dookie campus (−36.384 S, 145.707 E) from Sep-Oct 2019. A glasshouse day/night temperature cycle was maintained at $24 \pm 1/18 \pm 1$ °C with an average relative humidity of 65–70% (Izanloo et al. 2008). Photon flux intensity (measured at midday) was ~400 μmoles m^{-2} s^{-1} at the top of the plant canopy. During the experiment, the glasshouse received 11–12 hours of natural day light. One week after sowing, water-soluble ICL Peters Excel CalMag grower fertilizer containing 15% nitrogen (11.5% as NO_3-N, 2.1% as Ur-N, 1.4% as NH_4-N), 12.4% potassium (K), 2.2% phosphorus (P), 1.8% magnesium (Mg), 5.0% calcium (Ca), 0.12% iron (Fe), 0.02% boron (B), 0.06% manganese (Mn), 0.015% copper (Cu), 0.015% zinc (Zn) and 0.010% molybdenum (Mo) was applied to ensure recommended nutrient supply.

All pots were irrigated thrice a week with 85–90% field capacity to prevent excessive water drainage. Plant phenology was monitored daily using the Zadoks scale for the Z29 stage (before the start of pseudo-stem elongation) (Zadoks scale 29: Zadoks et al. 1974). At this stage, Si_0 and Si_1 group replicates were treated with two watering regimes, drought stress (DS, drought stress only; DSSi, drought stress on Si treated pots) where soil water content (SWC) was maintained at $38 \pm 3\%$ field capacity and control (CSi, silicon treatment control and C, absolute control) where SWC was maintained at 85–90% field capacity. Before the DS application, irrigation was gradually reduced for five to seven days for acclimation to attain $38 \pm 3\%$ field capacity. The relative humidity of the glasshouse was monitored for the whole growing cycle. Pots weights were taken daily to calculate the moisture loss by evapotranspiration and watered accordingly to maintain the field capacity of DS pots. During the experiment, pots were reshuffled every 2nd week to avoid pseudo replications and border effects.

Infrared thermal imaging-based computational water stress indices

On the 14th day of DS and before the termination of the experiment, infrared thermal images (IRTI) of each replicate were taken by using a high-performance thermal camera (T-series, Model 1050sc, FLIR Systems AB, Täby Sweden) (Fig. 1). Each IRTI Pixel holds a 16-bit thermal value in °C unit (FLIR T1050sc 2015). Infrared thermal images were taken from a constant 2 m distance and at a 30° angle from the horizontal. Every IRTI was taken in controlled glasshouse conditions at a temperature of 24 ± 1 °C to avoid canopy temperature acclimatization with the surrounding environment and to minimize the pixels temperature variations. All IRTI were converted to '.dat' format data files to extract temperature data using MATLAB code scripted in MATLAB R2017b (Math works Inc. Natick, Massachusetts, USA) and Images Analysis Toolbox (Fuentes et al. 2012; Mathworks 2017). While processing to calculate T_c and CWSI, the image background temperature effects were subtracted by setting the maximum and minimum thermal pixels within the canopy in the thermal histogram (Fuentes et al. 2012; Maes and Steppe 2012).

$$\text{CWSI} = \frac{(T_c - T_{wet})}{(T_{dry} - T_{wet})} \tag{2}$$

T_{wet} and T_{dry} are empirical reference temperatures estimated through statistical frequency analysis of IRTI (Fuentes et al. 2012).
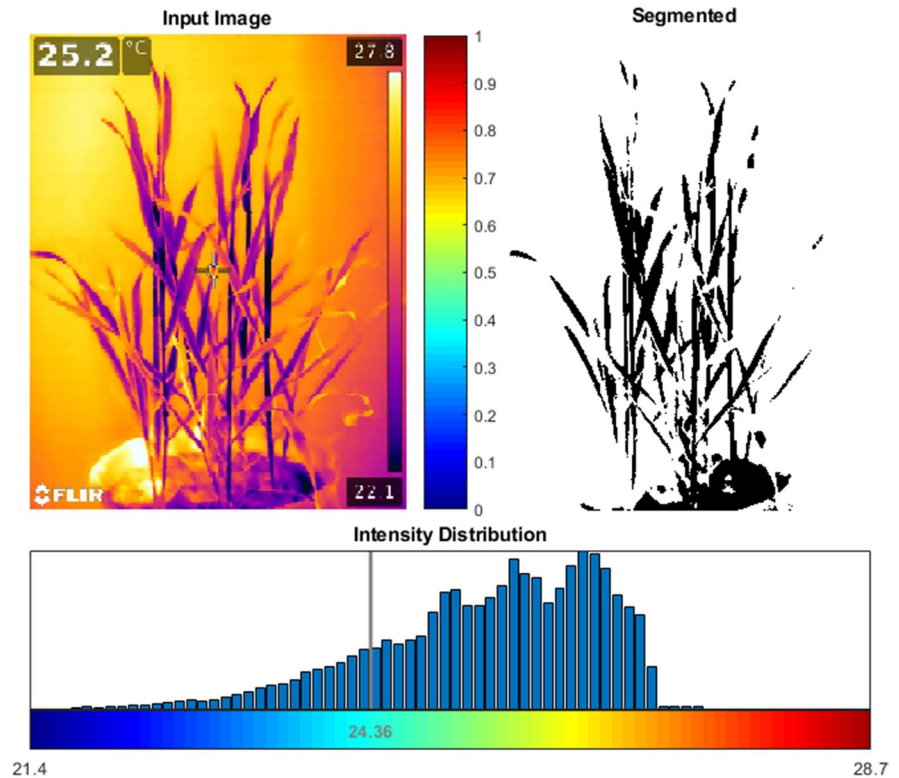
Using empirical reference temperature values and T_c, I_g was estimated by using eq. (3) as proposed by Fuentes et al. (2012) and Maes and Steppe (2012).

$$I_g = \frac{T_{dry} - T_c}{T_c - T_{wet}} = \frac{\gamma \, r_{av} + s \, r_{HR}}{\gamma \, r_s} \tag{3}$$

where 'r_{av}' is the resistance to vapor transfer in the boundary layer, 'γ' represents psychrometric constant, 's' is the curve slope relating temperature with saturated vapor pressure, 'r_s' is the stomatal resistance and "r_{HR}" is the parallel leaf resistance to the heat transfer and radiative heat loss.

CTD was also calculated from computational analysis of IRTI by subtracting the T_c from the mean

Fig. 1 Example of the image analysis graphic user interface showing the input thermal image (top left) and segmented binary image (top right) with the temperature intensity distribution (bottom) for the calculation of the representative canopy traits (canopy temperature, T_c; stomatal conductance index, I_g, canopy temperature depression, CTD; crop water stress index, CWSI and reference temperatures for stressed (T_{dry}) and non-stressed (T_{wet}) plants)

environmental temperature (T_a). It is positive when T_c is cooler than T_a, associated with different levels of transpiration (Balota et al. 2007).

$$CTD = T_a - T_c \tag{4}$$

Gaseous exchange measurements

On the last day of DS treatment, gaseous exchange measurements were recorded non-destructively using the flag leaf from each replicate. Photosynthesis (Pn), transpirational rate (E) and stomatal conductance (g_s) of flag leaves were recorded using a portable LICOR-6400 (LICOR, Lincoln, NE, USA). All the measurements were made between 09:30 and 11:30 a.m. under natural daylight conditions.

Plant sampling and harvest

Plants were harvested 14 days after being exposed to DS and 49 days after sowing. Fresh shoot weight (FW_S) was measured on a scale (± 0.01 g) in a glasshouse condition at the time of experiment

termination. Samples were then oven-dried at 70 °C for 72 hours and shoot dry weight (DW_S) was measured on a scale (± 0.001 g) under standard laboratory conditions.

Root crown scanning and image analysis

One uniformly grown plant was chosen from each pot for root traits measurement, and the stem was detached from the roots at the crown. The pots were briefly immersed in water, and the root crown was delicately washed with a water hose and nozzle to free them from debris and potting mix. Excess moisture on the root crowns was blotted with laboratory tissues and stored in 70% (v/v) alcohol at 4 °C until they were imaged to assess root morphological traits.

The root crown was carefully cut along the main axis for scanning, divided into 2–3 portions and spread evenly in a specialized root positioning tray (20×30 cm; made of translucent acrylic material) (Cai et al. 2015). A small paintbrush was used to gently separate primary and lateral roots and avoid overlapping or touching the tray edges. For roots to float and minimize overlap, the root positioning tray

was filled with 1–2 cm of water. The roots were then dual scanned with a flatbed scanner (Epson Perfection V800 Photo, Dual Lens System) for grayscale images. The transparent root positioning tray allows the roots to be scanned from above and below simultaneously to remove any noise or shadow effect on the root image. During the scanning process, water (scanning fluid) was changed regularly after every 2nd scan for clear images and to remove any noise from the previously scanned roots. The TIFF format grayscale root images were analyzed with RhizoVision Explorer at 400 dpi (Seethepalli and York 2020). The complete root system of each replication was scanned to avoid any associated errors. For root phenotyping and characterizing of cultivars under abiotic stress environments, root fragments with a diameter > 0.34 mm were selected for parameters related to primary roots. A segment with a diameter ≤ 0.34 mm was chosen for parameters related to lateral roots (Cai et al. 2015) (Fig. 2). Detailed descriptions of all the extracted root

crown traits used in this study are given in Table 1 of both Mattupalli et al. (2019) and Seethepalli et al. (2021) studies.

Statistical analysis

All statistical analysis and data graphics were created using R statistical software (R Core Team 2021) through the R integrated development environment RStudio (RStudio Team 2021). To determine how root's functional traits, IRTI water stress indices and gaseous exchange parameters of two contrasting wheat cultivars were performed in response to Si treatment under DS, a two-way ANOVA was performed ($p < 0.05$) to test the effects of Si treatment, DS and their interactions within the cultivars. Means and standard errors (SE) for all the studied traits were calculated using the 'dplyr' package of the R software (Wickham et al. 2021).
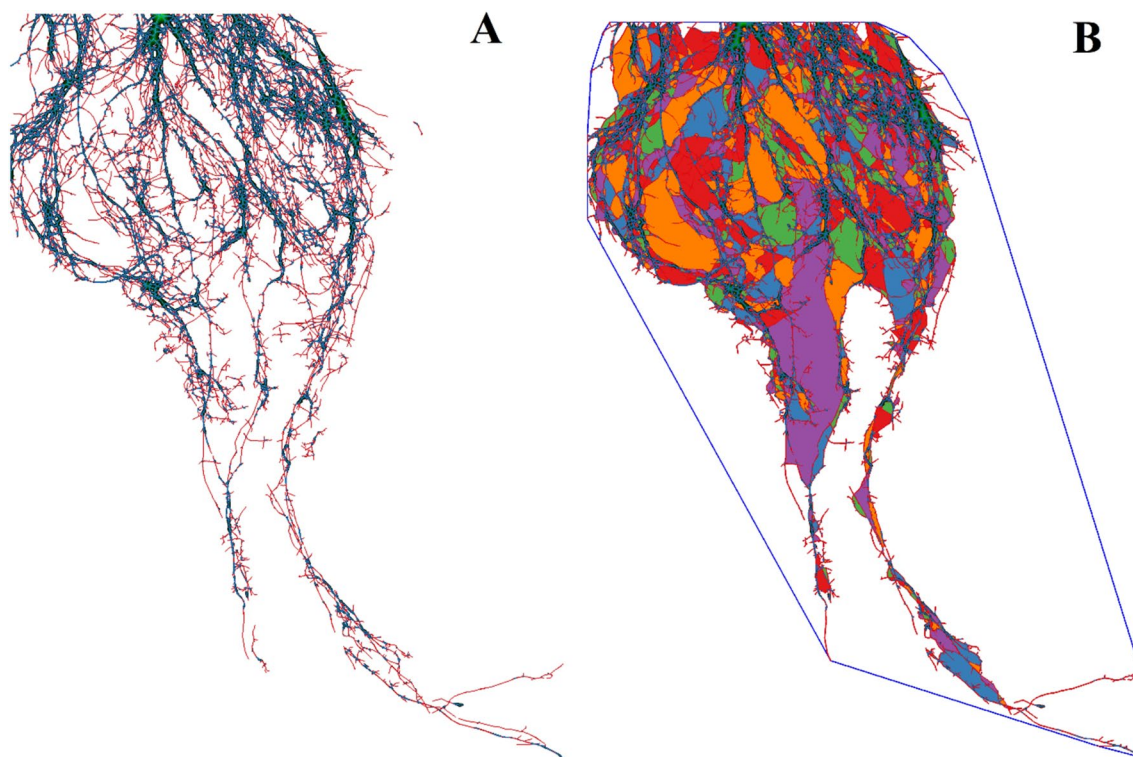

Fig. 2 Example of a representative segmented wheat root crown image, taken by RhizoVision Explorer; **A** showing primary roots (blue in colour, diameter with >0.34 mm) and lateral roots (red in colour, diameter with ≤0.34 mm) network and used to extract studied root features; **B** showing red outline within the root crown as root perimeter, multicolored boxes are representing holes in the root crown, and outer blue line covering the whole root system representing convex hull

To study the possible relationships or trade-offs among root morphological traits, water stress indices and gaseous exchange traits, scatter plot matrices for linear regression and correlation analysis for pairwise relationships were constructed by using the 'ggpairs' function of the 'GGally' package (Schloerke et al. 2021). To determine the multivariate ordination of studied traits for Si levels under DS, principal component analysis (PCA) was performed separately for each cultivar by using the 'prcomp' function of the default 'stats' package after centring and scaling the data. The 'ggplot2' package was used for plotting and data visualization.

Results

Effect of Si on root morphology under drought stress

The means and SE of root traits extracted from grey-scale images using RhizoVision Explorer root analyzer software are shown in Fig. 3. Results showed that Si treatment significantly ($p < 0.05$) improved most of the extracted root crown traits (except average diameter) from both cultivars under C and DS. Overall, root crowns, which were sampled from Si-treated pots, had significantly higher ($p < 0.001$) total root length (TRL) (Kukri-CSi, 32%; Kukri-DSSi, 58%; RAC875-CSi, 48%; RAC875-DSSi, 28%) than respective untreated pots (Fig. 3A).

Results showed that under CSi and DSSi, Si treatment significantly increased ($p < 0.001$) primary root length (PRL, roots with >0.34 mm in diameter) in both the cultivars when compared with respective untreated controls (C and DS, respectively). However, compared to Kukri, no significant effect of Si treatment was observed on the lateral root length (LRL, roots with ≤0.34 mm in diameter) of RAC875 under DSSi. The magnitude of the Si effect on PRL and LRL of RAC875 and Kukri was different. Under DSSi, Kukri, a susceptible cultivar, had a higher percent increase in PRL (44%) and LRL (28.1%) compared with RAC875 having a significant increase in PRL (35.2%) but a non-significant increase in LRL (Fig. 3B and C).

Interestingly, no significant effect ($p = 0.46$) of pre-sowing Si treatment was observed on the average diameter (AD) of root crowns in both RAC875 and Kukri under CSi and DSSi (Fig. 3D). Root tips (RT), an important indicator of root proliferation, were also calculated from root image analysis. Results showed that RT was significantly higher ($p < 0.01$) in both the cultivars under DSSi (RAC875, 13.1%; Kukri, 26.1%) when compared with respective DS pots (Fig. 3E).

Effect of Si on computational water stress indices under drought stress

Mean values ± SE of all the IRTI traits are presented in Fig. 4, showing a significant ($p < 0.05$) treatment effect on most of the traits. For T_c, compared to RAC875, a statistically significant difference was observed in Kukri under CSi when compared with absolute C. Under DS, an increase in T_c was observed for both cultivars. However, under DSSi, a significant reduction in T_c was recorded in Kukri (4.24%) and RAC875 (6.15%) in comparison with DS replicates of respective cultivars (Fig. 4A). Both cultivars had negative mean CTD values (eq. 4, RAC875, −1.96 °C; Kukri, −1.86 °C) under DS due to increased T_c and reduced transpiration (Fig. 4B). However, Si treatment significantly enhanced the CTD in both cultivars (RAC875, 78.6%; Kukri, 58.6%) under DSSi. Results showed that CWSI increased in RAC875 and Kukri under DS. Interestingly, no significant differences were observed in CWSI (eq. 2) in both the cultivars with Si and both watering treatments (C, CSi, DS, DSSi) (Fig. 4C). However, a decreasing trend was observed in RAC875 and Kukri, showing that Si reduced CWSI under DS conditions. The results also suggest that the CWSI threshold for both cultivars is still below the observed CWSI under controlled and drought-stressed conditions.

The automated IRTI statistical frequency analysis was also able to discriminate between reference leaves temperature data points for T_{dry} and T_{wet}. Variation in T_{wet} and T_{dry} can lead to variation in T_c. Although T_{wet} responses were significant under CSi for both cultivars, data did not show any significant differences in T_{dry} of both the cultivars under CSi treatment when compared with their respective Cs. Reference leaves temperature (T_{dry} and T_{wet}), calculated from Si-treated replicates of both cultivars, had significantly lower values under DSSi when compared with respective DS (Fig. 4D and E). T_{dry} and T_{wet} were also used to calculate the I_g (eq. 3) through the leaf energy balance, an important physiological attribute that is directly
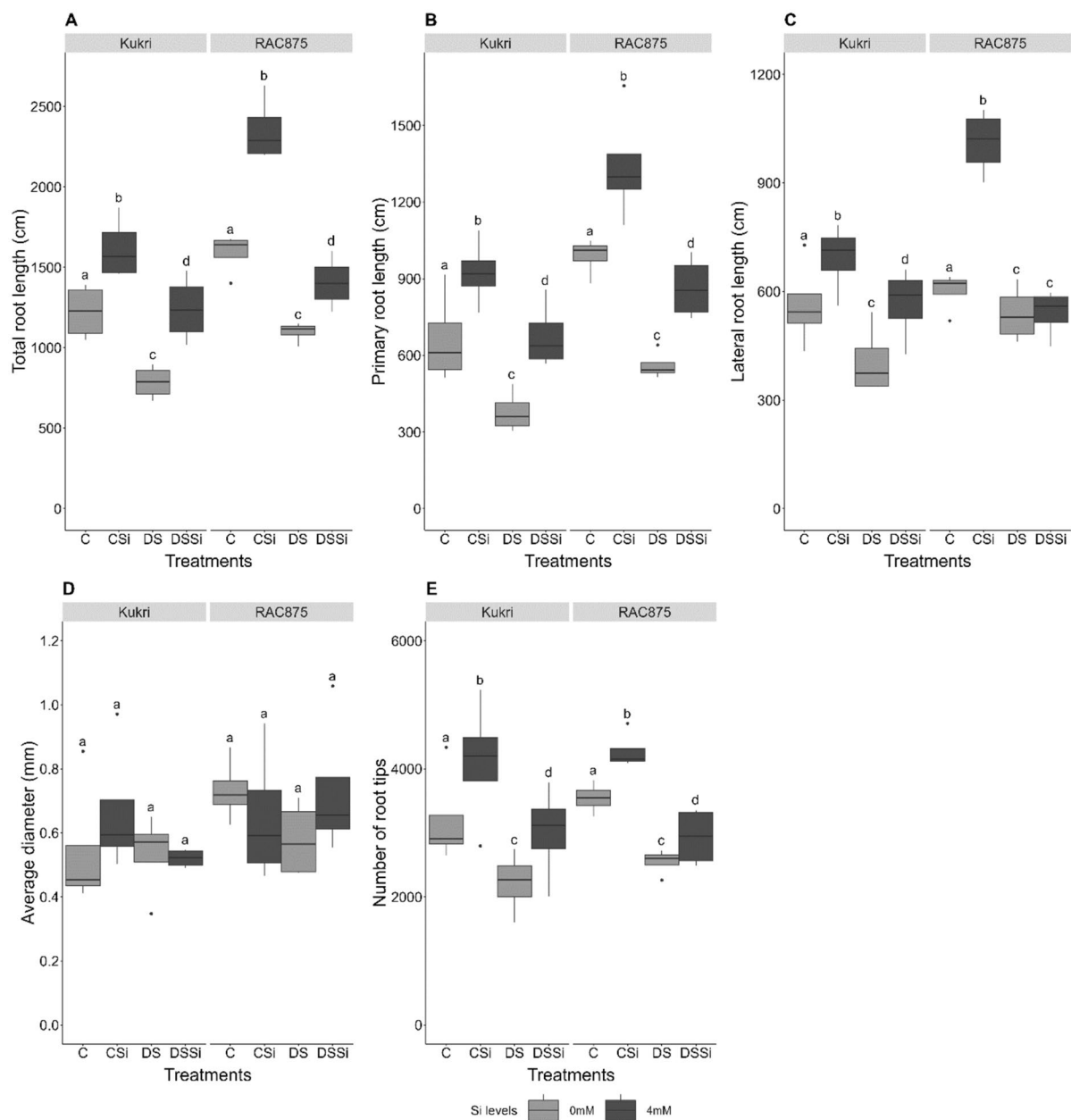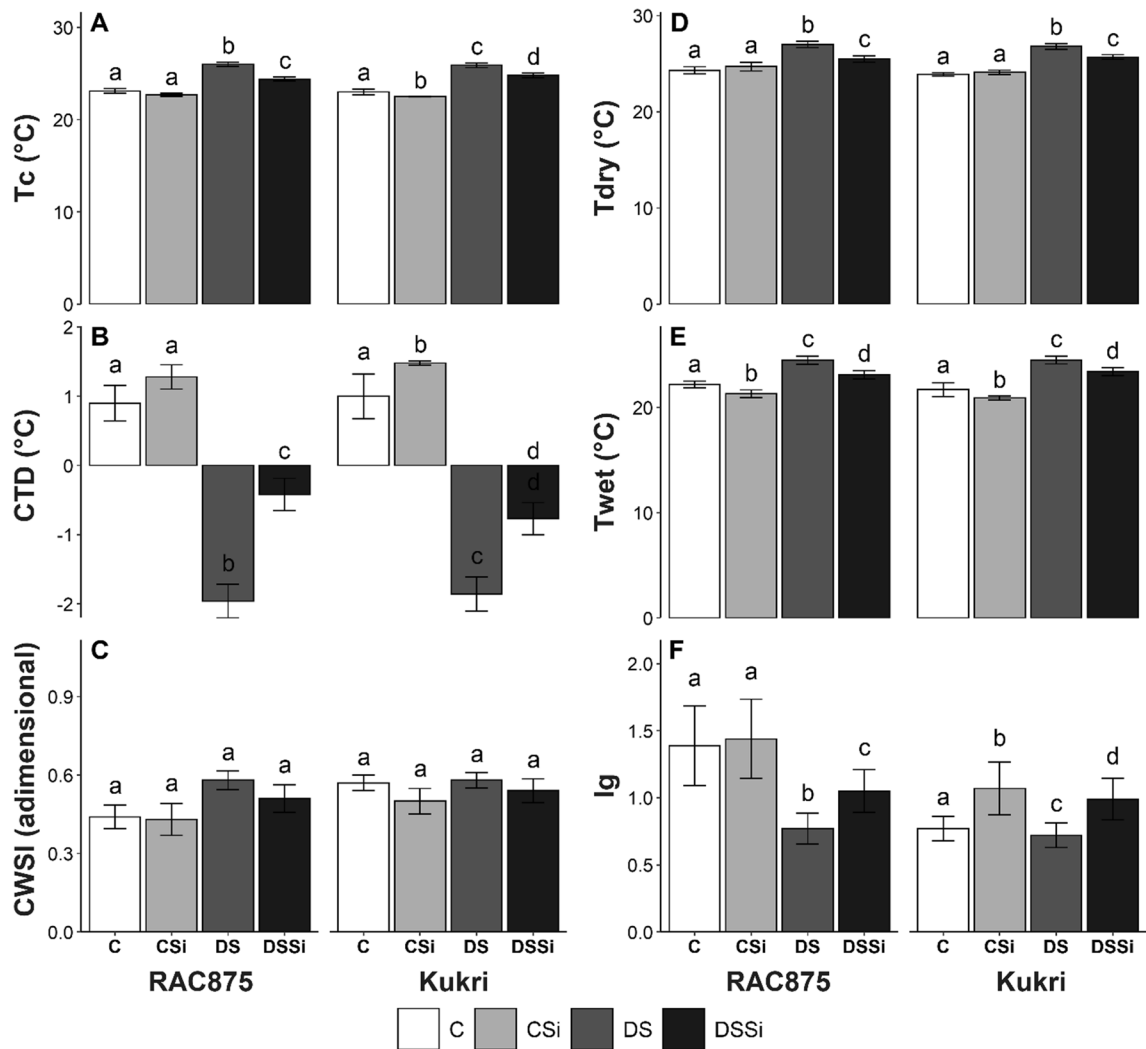
Fig. 3 Effect of silicon on various extracted root traits of two contrasting wheat cultivars (RAC875 and Kukri) under control and drought stress. Values are given as means ± SE of four replicates. Statistical comparisons were performed within each cultivar. Different letters on error bars within each treatment denote the significant effect of silicon ($p < 0.05$)

proportional to g_s. In RAC875, a non-significant effect of Si was observed in I_g under CSi, compared with Kukri in the same treatment. Representative data showed that Si treatment significantly increased I_g in both the cultivars under DSSi treatment compared with respective DS controls. The percent increase in I_g was almost the same in both Kukri (27.3%) and RAC875 (26.7%) under DSSi (Fig. 4F).

Fig. 4 Effect of silicon on water stress indices of two contrasting wheat cultivars (RAC875 and Kukri) under control and drought stress. Values are given as means ± SE of four replicates. Statistical comparisons were performed within each cultivar. Different letters on error bars within each treatment denote the significant effect of silicon ($p < 0.05$). **A**. canopy temperature (T_c); **B**. canopy temperature depression (CTD); **C**. crop water stress index (CWSI); **D**. reference temperature for the stressed plant (T_{dry}); **E**. reference temperature for the non-stressed plant (T_{wet}); **F**. stomatal conductance index (I_g)

Effect of Si on gaseous exchange traits under drought stress

Except for P_n in Kukri, gaseous exchange traits (P_n, g_s, E) were non-significant under control with Si treatment (Fig. 5). Under DS, a significant decrease was observed in the P_n of both cultivars (Kukri, 60%; RAC875, 53.2%) compared to the respective controls of each cultivar. However, Si treatment substantially reduced this decline (Kukri, 40.2%; RAC875, 30.6%)

and led to a significant increase ($p < 0.05$) (Fig. 5A). Silicon treatment did not significantly change g_s under CSi in both cultivars. Under DSSi, however, Si-treated Kukri and RAC875 plants exhibited substantially higher g_s (Kukri, 26.8%; RAC875, 26.6%) than the respective DS replicates ($p < 0.05$) (Fig. 5B). Similarly, Si treatment did not significantly change leaf transpiration of both the cultivars under CSi, whereas, under DSSi, Si-treated plants of Kukri and RAC875 had significantly higher transpirational rates
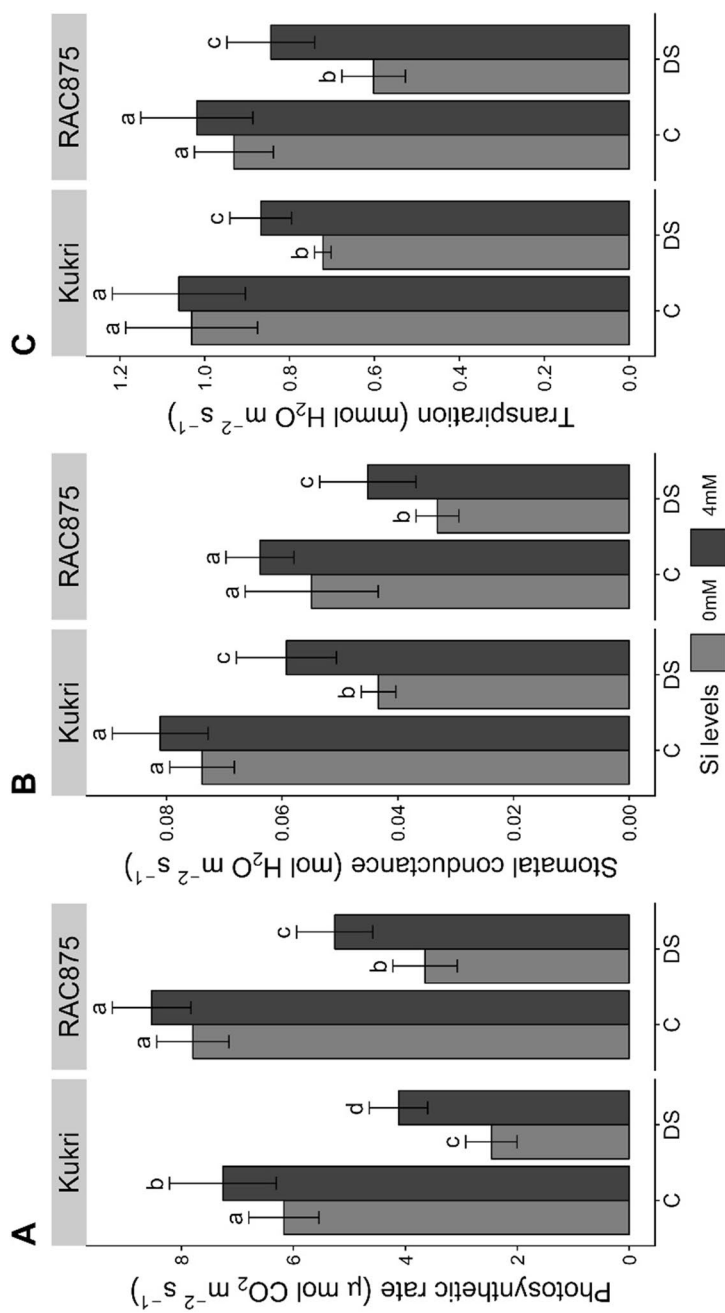
Fig. 5 Effect of silicon on gaseous exchange traits of two contrasting wheat cultivars (RAC875 and Kukri) under control and drought stress. Values are given as means ± SE of four replicates. Statistical comparisons were performed within each cultivar. Different letters on error bars within each treatment denote the significant effect of silicon ($p < 0.05$)

(Kukri, 16.9%; RAC875, 28.7%) than in the DS replicates (Fig. 5C). These results showed that exogenous Si treatment could enhance gaseous exchange traits of drought-tolerant and drought-susceptible wheat cultivars under controlled drought stress conditions.

Relationship among root traits, water stress indices and gaseous exchange parameters

From the studied traits, a Pearson correlation matrix was established for each cultivar using a set of nine statistically significant traits from root image analysis, IRTI water stress indices and gaseous exchange traits to identify correlation among these independent traits (Fig. 6). Scatter plot matrices for RAC875 and Kukri showed that Si-induced TRL had a strong positive correlation with LRL (RAC875, $p < 8.4\mathrm{e}^{-04}$; Kukri, $p < 3.1\mathrm{e}^{-03}$) and PRL (RAC875, $p < 3.3\mathrm{e}^{-04}$, Kukri, $p < 1.8\mathrm{e}^{-04}$) as compared to control (Fig. 6A and B, upper panel). Results showed that TRL has a linear increase with PRL and LRL under DSSi (Fig. 6A and B, lower panel). Similarly, results from Si-treated replicates under DS showed that PRL and LRL have a strong positive association with each other in both the cultivars (RAC875, $p < 0.02$; Kukri, $p < 0.04$) as compared with untreated controls (RAC875, $p = 2.1$; Kukri, $p = 4.7$).

Data showed that T_c is strongly influenced by root traits in both cultivars and showed a negative correlation. T_c also showed a strong negative association with CTD under control and Si-treated DS replicates in both the cultivars (Fig. 6A and B, lower panel). However, no significant relationship of root traits (except PRL in RAC875) was found with calculated I_g both under Si treated (CSi & DSSi) and control (C & DS) replicates (Fig. 6A and B, upper panel). Si-induced root traits significantly enhanced CTD in RAC875 (TRL, $p < 0.003$; LRL, $p < 0.002$; PRL, $p < 0.02$) and Kukri (TRL, $p < 0.03$; PRL, $p < 0.03$). Among gaseous exchange traits, the panel showed that P_n is linearly enhanced with the increase in Si-induced root traits in Kukri compared with RAC875 under DSSi (Fig. 6A and B, upper and lower panel).

Multivariate analysis

Principal component analysis (PCA) was performed on root crown traits, computational water stress indices, P_n and E (g_s not presented due to lower explained variance on the factor map) of each cultivar under drought and Si treatment effect (Fig. 7). The PCAs obtained from the standardized cultivar-by-traits data matrix of RAC875 and Kukri explained a total cumulative variance of 80.9% (PC1 = 63.3% and PC2 = 17.6%) and 78.6% (PC1 = 56.7% and PC2 = 21.9%), respectively for the first two principal components. Replicated data was used to construct PCA to better represent variance from the data set. As per the rotated PCA matrix of RAC875 (Fig. 7A) and Kukri (Fig. 7B), PC1 was greatly influenced by TRL, PRL, LRL, and RT with a higher positive factor loading on the factor map, suggesting that these four independent variables vary together with Si effect. In contrast, PC2 was greatly influenced by the P_n and I_g with higher positive factor loading on the factor map. The biplot ordination of RAC875 and Kukri exhibited distinct separation, showing Si's positive contribution to overall root crown traits, computational water stress indices, and P_n under drought stress treatment.

The loading of vectors on the PCA plots (Fig. 7A, B) also illustrates the relationship among different variables. The corresponding vectors of variables with an angle of <90° show a positive relationship, and corresponding vectors of variables with an angle of >90° show a negative association with each other. Among the loaded traits on PCA factor maps, a group of highly correlated variables, i.e., TRL and PRL, contributed the most to the P_n in both cultivars with the Si effect. Due to the obtuse angle on the factor map, it is also shown that Si-induced TRL, PRL, and LRL positively contributed to maintaining the T_c and CWSI at a lower level in both cultivars under drought stress.

Discussion

Several pieces of research have shown that Si has a positive impact on alleviating drought stress through different physiological mechanisms, including various osmotic adjustments, enhanced antioxidant responses, modification in gas exchange attributes, and regulation of compatible solutes (Alzahrani et al. 2018; Debona et al. 2017; Ashfaq et al. 2022). Previously reported literature showed that applying 4 mM silicic acid salt mitigated abiotic stress effects effectively (Alzahrani et al. 2018; Ashfaq et al. 2022). The current study presented a novel analysis of Si-induced
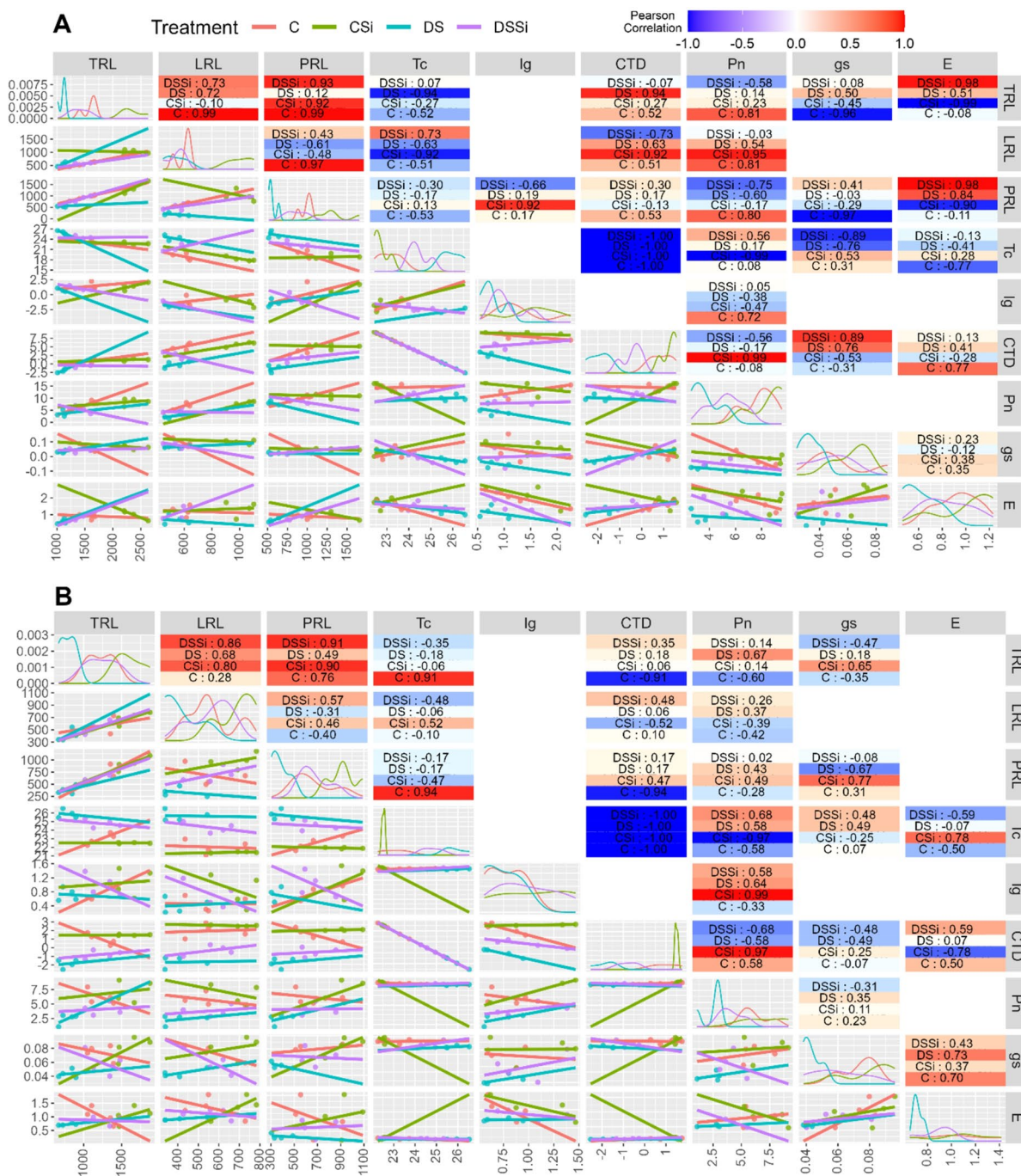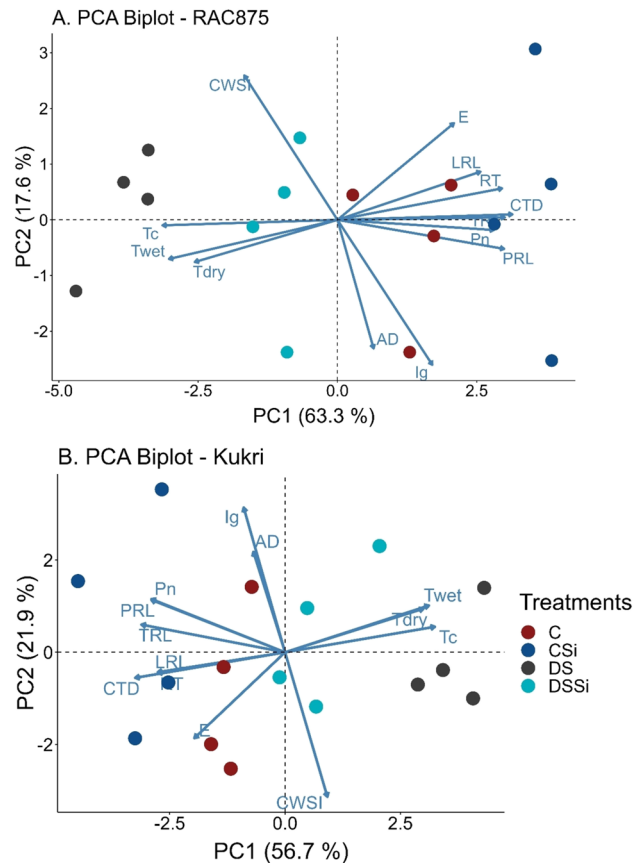
Fig. 6 Scatter plot matrix showing a relationship among extracted root traits, infrared thermal imaging water stress indices and gaseous exchange parameters of (**A**) RAC875 and (**B**) Kukri under silicon (Si) and drought stress treatments. The lower panel of the plot showed linear pairwise regression, and the upper panel of the plot showed a correlation among plotted root traits, IRTI water stress indices and gaseous exchange traits. The correlation matrix only shows significant correlation values at $p \leq 0.05$, leaving non-significant boxes empty. Asterisks highlight the level of significance according to p values ("***" if p value <0.001, "**" if p value <0.01, "*" if p value <0.05). Abbreviations are total root length (TRL), lateral root length (LRL), primary root length (PRL), canopy temperature (T_c), stomatal conductance index (I_g), canopy temperature depression (CTD), photosynthesis (P_n), stomatal conductance (g_s) and transpiration (**E**)

Fig. 7 The PCA biplot for extracted root crown traits, computational water stress indices, leaf transpiration and photosynthesis of (**A**) RAC875 and (**B**) Kukri under drought and silicon treatment effects. Abbreviations are total root length (TRL), primary root length (PRL), lateral root length (LRL), average diameter (AD), root tips (RT), canopy temperature (T_c), stomatal conductance index (I_g), canopy temperature depression (CTD), crop water stress index (CWSI), reference temperature for the stressed (T_{dry}) and non-stressed plants (T_{wet}), photosynthesis (P_n), transpirational rate (E)

improvement in root system components of two contrasting bread wheat cultivars that would potentially correlate to cooler canopy traits and higher photosynthetic efficiency in drought-stressed conditions.

Characterizing root traits and their implications for final grain yield

The current study showed that Si treatment facilitated overall root growth irrespective of water availability and drought tolerance status of the studied wheat cultivars (Fig. 3A, B and C). Comparing both cultivars revealed that the percent increase in root traits was higher in Kukri (susceptible cultivar) than in RAC875 (tolerant cultivar). The observed improvements in the root traits of contrasting wheat cultivars may be due to the positive effects of Si leading to better water relations, photosynthetic efficiency (Debona et al. 2017), and ultimately, above and below-ground

plant growth (Steinemann et al. 2015). Cultivars with extended and deep root systems can better utilize subsoil moisture at the onset of drought to meet evapotranspiration demand (Lynch and Wojciechowski 2015; Wasson et al. 2012) and helpful in conserving more moisture and nutrients for the reproductive phase (Palta et al. 2011). The early root growth and rooting depth correlate positively to post-anthesis water use, facilitating faster crop establishment, leaf area development and shoot biomass increment at later growth stages (Lynch and Wojciechowski 2015). The exact mechanisms for Si-induced root growth in both cultivars are not known. However, Yin et al. (2014) previously reported that Si regulates 1-aminocyclopropane-1-carboxylic acid (the precursor of ethylene) and polyamine levels under drought to enhance root growth and root/shoot ratio, thus contributing to increased water uptake. Such Si-induced modulations in root development also lead to silica aggregation in

the root endodermal cell walls. Endodermal silicification contributes positively by decreasing root growth inhibition followed by desiccation (Soukup et al. 2017).

Soil compaction due to dry period becomes a significant limiting factor for roots to proliferate and ultimately reduces crop productivity. Higher root tip number due to improved root branching indicates better root proliferation, which could be beneficial for the plants growing under water limited environments Previously, Colombi et al. (2017) explained how root tips and root diameter can positively influence root penetration under different soil strengths. In the current study, Si treatment positively increased the root tips of both wheat cultivars under well-water and drought conditions. However, studies showed that root tip geometry must also be considered when referring to root tips for drought studies (Colombi et al. 2017). A smaller root tip radius is desirable, enabling a higher root elongation in compact soil. Further experimentations are required to see the possible effect of Si treatment on root tips through detailed studies on root tip diameter under drought stress. The current study also found that the pre-sowing Si treatment has a non-significant effect on the calculated average root diameter in both cultivars, irrespective of soil moisture availability. This might be because the increase in root diameters is controlled by the genotypic architecture and independent of Si treatment affect (Liu et al. 2014). Previously it was reported that an increase in root diameter was not a desirable trait, and roots with higher TRL with smaller root diameter at depth are more adapted to drought-stress environments (Schoppach et al. 2013).

Gaseous exchange traits

Drought stress causes severe disruptions to the plant photosynthetic system and, therefore, the photosynthetic flux. The plant's ability to maintain higher photosynthesis is interlinked with vigorous root system, especially in a water-limited environment (Cattivelli et al. 2008), as shown in Figs. 7A and B. A deep and vigorous rooting system contributes to drought avoidance by enabling access to subsoil moisture and facilitating higher transpiration for cooler canopies and better photosynthesis under drought stress (Kulkarni et al. 2017). Wheat root system growth is stimulated through the daily allocation of photosynthetic carbon

during the early growth stages. In the current study, gaseous exchange traits were significantly decreased with drought stress. Still, Si significantly reduced this decrease in drought-tolerant and susceptible wheat cultivars (Fig. 5A, B and C). The Si-induced increase in net photosynthesis might be due to up-regulation of key genes expressions related to photosynthesis with Si addition (Detmann et al. 2012). The other possible reason for the increase in net photosynthesis would be increased leaf erectness after Si treatment, which in turn reduce leaf-shading for better light transmittance (Tamai and Ma 2008). The Detmann et al. (2012) concluded that Si application stimulates source capacity coupled with higher sink demand which in turn improves nitrogen remobilization for higher grain yield in rice.

Previously, it was reported that stomatal conductance and maximal photosynthesis positively correlated with higher grain yield, especially under drought (Cattivelli et al. 2008). Various research studies have attempted to investigate the mechanistic bases of photosynthesis and the stomatal conductance relationship, but the underlying mechanisms are still unclear (Detmann et al. 2012). Stomatal conductance regulation mostly depends on leaf and mesophyll cell wall thickness. In the current study, Si has shown an influence on regulating stomatal conductance under drought. Silicon interacts with several endogenous phytohormones, including abscisic acid (ABA), to improve stress tolerance. ABA plays a major role in cellular signaling and it was reported that Si application regulates the ABA biosynthesis through transcription of PYL1, PYL4, and PYR8 genes and enhances the stomatal conductance and other gaseous exchange traits (Arif et al. 2021).

Crop water stress indices

Most remote sensing techniques have been used to indirectly study plant water status by estimating crop water stress indices (T_c, CTD, CWSI). The current study revealed the genotypic differences in drought stress tolerance as detected by IRTI. Canopy temperature is an important physiological attribute related to plant water status and other metabolic processes like gaseous exchange traits (Biju et al. 2018; Maes and Steppe 2012). Normally, T_c is determined by the evaporative cooling via leaf transpiration, which is a control-feedback function among stomatal

conductance and root hydraulic conductivity (Ober et al. 2021). However, during drought stress or when atmospheric demand for transpiration increases, T_c is primarily a function of root system capacity to supply enough water to meet transpiration demand. Current study results revealed that under control, both RAC875 and Kukri continue to transpire through open stomata to maintain T_c (Biju et al. 2018). Under severe drought, stomatal closure to control leaf transpiration is a common plant response, ultimately increasing T_c (Fig. 4A). However, under DSSi, a higher percent decrease in T_c in a susceptible cultivar might be due to increased stomatal conductance for enhanced transpiration compared to a tolerant cultivar (Fig. 5B, C), as previously reported by Detmann et al. (2012) and Hossain et al. (2002).

Canopy temperature depression is a measure of transpirational efficiency and has been used for the phenotyping of crops under environmental stresses, especially drought (Biju et al. 2018; Kumar et al. 2017; Maes and Steppe 2012). The current study showed that CTD decreased with the increase in DS and was negative in both cultivars. However, under DSSi, CTD in RAC875 and Kukri is significantly enhanced. This means that after Si treatment, both cultivars adapted more to DS by conserving extra moisture in their tissues due to the Si-induced extended root system (Fig. 3) and improved root hydraulic conductivity. The CWSI is the most commonly used thermal drought stress index and is closely correlated with the soil moisture level, leaf water potential and evapotranspiration (Maes and Steppe 2012). In the current study, drought severity tends to be a notable increase in CWSI in both cultivars (Fig. 4C). Previously, Biju et al. (2018) reported that CWSI increases in lentil cultivars with the severity of drought stress. Results showed that Si-treated replicates had improved their water status under drought, and it is within the expectation as exhibited with lower CWSI values. Although grain yield was not part of this study. However, a decrease in CWSI with Si treatment might be linked with improved biomass and grain yield.

The stomatal conductance index, estimated through IRTI, uses the same leaf scale input data as CWSI, and it is correlated with stomatal conductance, provided T_a, wind speed, and constant factor (G) relating to g_s, and I_g remain constant (Maes and Steppe 2012). They also reported that g_s rapidly

respond to the changing leaf water status by regulating various gas exchange fluxes for maximum photosynthesis and controlling T_c. As wind varied little in the current study, a positive linear relationship was observed between stomatal conductance and I_g (Fig. 6A and B). As shown in Fig. 5B, both cultivars have a significant increase in stomatal conductance, as demonstrated by a substantial increase in I_g under DSSi. Still, I_g was higher in the susceptible cultivar (Fig. 4F). These results are consistent with previous findings stating I_g and g_s showed a linear relationship in various horticultural crops, including grapevines (Fuentes et al. 2012) and olive trees (Egea et al. 2017).

Multivariate data analysis

The PCA results from RAC875 (Fig. 7A), and Kukri (Fig. 7B) are in agreement with the criteria set by Sneath and Sokal (1973) that PC1 and PC2 must explain at least 70% of the total explained variation to avoid overfitting. The length of plotted traits eigenvectors explained the quality of representation on the factor map. The loading of plots for both cultivars shows the extent of the relationship between the original variables and respective PCs. The PC1 of RAC875 and PC2 of Kukri strongly correlated with root length, gaseous exchange traits and CTD, suggesting that these independent variables were intercorrelated, showing positive association. In both cultivars, the TRL was highly dependent on PRL and LRL, which improved CTD and P_n under drought stress. As reported in this study, T_c is primarily a function of the root system's capacity to supply enough water to meet transpiration demand to enhance P_n. Overall, the results suggest that Si treatment regulated the water stress indices and photosynthetic activity, translating into improved canopy physiology and higher crop growth, including root characteristics under drought stress.

Conclusion

This study suggests that Si enhances root functional traits for moisture and nutrient uptake with improved photosynthesis, stomatal conductance, transpiration and computational crop water stress indices in a drought-stress environment. Thus, along with the drought-tolerant cultivar, the beneficial role of Si

in stimulating root growth and mitigating drought stress at early growth stages was also confirmed in the drought-susceptible cultivar. Overall, the current study demonstrates that pre-sowing Si treatment improves wheat adaptability by upregulating plant physiological traits and provides a basis for further studies about the role of Si in regulating root-sourced chemical signalling and other physiological attributes under terminal and intermittent drought stress, both in controlled and field conditions.

Data availability The data supporting this study's findings are available from the corresponding author upon reasonable request.

Declarations

References

Alzahrani Y, Kuşvuran A, Alharby HF, Kuşvuran S, Rady MM (2018) The defensive role of silicon in wheat against stress conditions induced by drought, salinity or cadmium. Ecotoxicol Environ Saf 154:187–196

Arif Y, Singh P, Bajguz A, Alam P, Hayat S (2021) Silicon mediated abiotic stress tolerance in plants using physio-biochemical, omic approach and cross-talk with phytohormones. Plant Physiol Biochem 166:278–289

Ashfaq W, Fuentes S, Brodie G, Gupta D (2022) The role of silicon in regulating physiological and biochemical mechanisms of contrasting bread wheat cultivars under terminal drought and heat stress environments. Front Plant Sci 13

Balota M, Payne WA, Evett SR, Lazar MD (2007) Canopy temperature depression sampling to assess grain yield and genotypic differentiation in winter wheat. Crop Sci 47:1518–1529

Bao Y, Aggarwal P, Robbins NE, Sturrock CJ, Thompson MC, Tan HQ, Tham C, Duan L, Rodriguez PL, Vernoux T (2014) Plant roots use a patterning mechanism to position lateral root branches toward available water. Proc Natl Acad Sci 111:9319–9324

Bennett D, Reynolds M, Mullan D, Izanloo A, Kuchel H, Langridge P, Schnurbusch T (2012) Detection of two major grain yield QTL in bread wheat (Triticum aestivum L.) under heat, drought and high yield potential environments. Theor Appl Genet 125:1473–1485

Biju S, Fuentes S, Gupta D (2017) Silicon improves seed germination and alleviates drought stress in lentil crops by regulating osmolytes, hydrolytic enzymes and antioxidant defense system. Plant Physiol Biochem 119:250–264

Biju S, Fuentes S, Gupta D (2018) The use of infrared thermal imaging as a non-destructive screening tool for identifying drought-tolerant lentil genotypes. Plant Physiol Biochem 127:11–24

Bishopp A, Lynch JP (2015) The hidden half of crop yields. Nat Plants 1:1–2

Cai J, Zeng Z, Connor JN, Huang CY, Melino V, Kumar P, Miklavcic SJ (2015) RootGraph: a graphic optimization tool for automated image analysis of plant roots. J Exp Bot 66:6551–6562

Cattivelli L, Rizza F, Badeck F-W, Mazzucotelli E, Mastrangelo AM, Francia E, Marè C, Tondelli A, Stanca AM (2008) Drought tolerance improvement in crop plants: an integrated view from breeding to genomics. Field Crop Res 105:1–14

Colombi T, Kirchgessner N, Walter A, Keller T (2017) Root tip shape governs root elongation rate under increased soil strength. Plant Physiol 174:2289–2301

Debona D, Rodrigues FA, Datnoff LE (2017) Silicon's role in abiotic and biotic plant stresses. Annu Rev Phytopathol 55:85–107

Detmann KC, Araújo WL, Martins SC, Sanglard LM, Reis JV, Detmann E, Rodrigues FÁ, Nunes-Nesi A, Fernie AR, Damatta FM (2012) Silicon nutrition increases grain yield, which, in turn, exerts a feed-forward stimulation of photosynthetic rates via enhanced mesophyll conductance and alters primary metabolism in rice. New Phytol 196:752–762

Egea G, Padilla-Díaz CM, Martinez-Guanter J, Fernández JE, Pérez-Ruiz M (2017) Assessing a crop water stress index derived from aerial thermal imaging and infrared thermometry in super-high density olive orchards. Agric Water Manag 187:210–221

Fleury D, Jefferies S, Kuchel H, Langridge P (2010) Genetic and genomic tools to improve drought tolerance in wheat. J Exp Bot 61:3211–3222

FLIR T1050SC (2015) FLIR T1050sc: HD Thermal Imaging For R&D Applications. FLIR Systems, Inc. Available at: http://www.flirmedia.com/MMC/THG/Brochures/RND_055/RND_055_APAC.pdf. Accessed 1 Nov 2019

Fuentes S, de Bei R, Pech J, Tyerman S (2012) Computational water stress indices obtained from thermal image analysis of grapevine canopies. Irrig Sci 30:523–536

Hossain MT, Mori R, Soga K, Wakabayashi K, Kamisaka S, Fujii S, Yamamoto R, Hoson T (2002) Growth promotion and an increase in cell wall extensibility by silicon in rice and some other Poaceae seedlings. J Plant Res 115:0023–0027

IPCC (2019) Food security. In: Shukla PR, Skea J, Calvo Buendia E, Masson-Delmotte V, Pörtner H-O, Roberts DC, Zhai P, Slade R, Connors S, van Diemen R, Ferrat M, Haughey E, Luz S, Neogi S, Pathak M, Petzold J, Portugal Pereira J, Vyas P, Huntley E, Kissick K, Belkacemi M, Malley J (eds) Climate change and land: an IPCC special report on climate change, desertification, land degradation, sustainable land management, food security, and greenhouse gas fluxes in terrestrial ecosystems. https://doi.org/10.1017/9781009157988.007

Izanloo A, Condon AG, Langridge P, Tester M, Schnurbusch T (2008) Different mechanisms of adaptation to cyclic water stress in two south Australian bread wheat cultivars. J Exp Bot 59:3327–3346

Khadka K, Earl HJ, Raizada MN, Navabi A (2020) A physio-morphological trait-based approach for breeding drought tolerant wheat. Front Plant Sci 11:715

Kulkarni M, Soolanayakanahally R, Ogawa S, Uga Y, Selvaraj MG, Kagale S (2017) Drought response in wheat: key genes and regulatory mechanisms controlling root system architecture and transpiration efficiency. Front Chem 5:106. https://doi.org/10.3389/fchem.2017.00106

Kumar M, Govindasamy V, Rane J, Singh A, Choudhary R, Raina S, George P, Aher L, Singh N (2017) Canopy temperature depression (CTD) and canopy greenness associated with variation in seed yield of soybean genotypes grown in semi-arid environment. S Afr J Bot 113:230–238

Liang Y, Hua H, Zhu YG, Zhang J, Cheng C, Römheld V (2006) Importance of plant species and external silicon concentration to active silicon uptake and transport. New Phytol 172:63–72

Lilley J, Kirkegaard J (2011) Benefits of increased soil exploration by wheat roots. Field Crop Res 122:118–130

Liu P, Yin L, Deng X, Wang S, Tanaka K, Zhang S (2014) Aquaporin-mediated increase in root hydraulic conductance is involved in silicon-induced improved root water uptake under osmotic stress in Sorghum bicolor L. J Exp Bot 65:4747–4756

Luyckx M, Hausman J-F, Lutts S, Guerriero G (2017) Silicon and plants: current knowledge and technological perspectives. Front Plant Sci 8:411

Lynch JP, Wojciechowski T (2015) Opportunities and challenges in the subsoil: pathways to deeper rooted crops. J Exp Bot 66:2199–2210

Maes W, Steppe K (2012) Estimating evapotranspiration and drought stress with ground-based thermal remote sensing in agriculture: a review. J Exp Bot 63:4671–4712

Mathworks M (2017) MATLAB and statistics toolbox release. The MathWorks. Inc, Natick, MA

Mattupalli C, Seethepalli A, York LM, Young CA (2019) Digital imaging to evaluate root system architectural changes associated with soil biotic factors. Phytobiomes J 3:102–111

Meister R, Rajani M, Ruzicka D, Schachtman DP (2014) Challenges of modifying root traits in crops for agriculture. Trends Plant Sci 19:779–788

Ober ES, Alahmad S, Cockram J et al (2021) Wheat root systems as a breeding target for climate resilience. Theor Appl Genet 134(6):1645–1662. https://doi.org/10.1007/s00122-021-03819-w

Palta JA, Chen X, Milroy SP, Rebetzke GJ, Dreccer MF, Watt M (2011) Large root systems: are they useful in adapting wheat to dry environments? Funct Plant Biol 38:347–354

Pepper I, Brusseau M (2019) Chapter 2 - Physical-chemical characteristics of soils and the subsurface. Environ Pollut Sci, 9–22. https://doi.org/10.1016/B978-0-12-814719-1.00002-1

R Core Team (2021) R: A language and environment for statistical computing. R Foundation for Statistical Computing, Vienna, Austria. URL https://www.R-project.org/

Raza A, Mubarik MS, Sharif R, Habib M, Jabeen W, Zhang C, Chen H, Chen ZH, Siddique KH, Zhuang W (2023) Developing drought-smart, ready-to-grow future crops. The Plant Genome 16:e20279

RStudio Team (2021) RStudio: Integrated Development Environment for R. RStudio, PBC, Boston, MA. URL http://www.rstudio.com/

Schloerke B, Cook D, Larmarange J, Briatte F, Marbach M, Thoen E, Elberg A, Crowley J (2021) GGally: Extension to 'ggplot2'. GGally: Extension to 'ggplot2'. R package version 2.1.1. https://CRAN.R-project.org/package=GGally

Schoppach R, Wauthelet D, Jeanguenin L, Sadok W (2013) Conservative water use under high evaporative demand associated with smaller root metaxylem and limited trans-membrane water transport in wheat. Funct Plant Biol 41:257–269

Seethepalli A, York L (2020) RhizoVision explorer—interactive software for generalized root image analysis designed for everyone (version 2.0.2). Zenodo. https://doi.org/10.5281/zenodo.4095629

Seethepalli A, Dhakal K, Griffiths M, Guo H, Freschet GT, York LM (2021) RhizoVision Explorer: Open-source software for root image analysis and measurement standardization. AoB plants, 13, plab056. https://doi.org/10.1093/aobpla/plab056

Sneath PH, Sokal RR (1973) Numerical taxonomy. The principles and practice of numerical classification. WH Freeman Co, San Francisco, CA

Soukup M, Martinka M, Bosnić D, Čaplovičová M, Elbaum R, Lux A (2017) Formation of silica aggregates in sorghum root endodermis is predetermined by cell wall architecture and development. Ann Bot 120:739–753

Souri Z, Khanna K, Karimi N, Ahmad P (2021) Silicon and plants: current knowledge and future prospects. J Plant Growth Regul 40:906–925

Steinemann S, Zeng Z, McKay A, Heuer S, Langridge P, Huang CY (2015) Dynamic root responses to drought and rewatering in two wheat (Triticum aestivum) genotypes. Plant Soil 391:139–152

Tamai K, Ma JF (2008) Reexamination of silicon effects on rice growth and production under field conditions using a low silicon mutant. Plant Soil 307:21–27

Tang L, Tan F, Jiang H, Lei X, Cao W, Zhu Y (2011) Root architecture modeling and visualization in wheat. Computer and Computing Technologies in Agriculture IV: 4th IFIP TC 12 Conference, CCTA 2010, Nanchang, China, October 22–25, 2010, Selected Papers, Part II 4. Springer, 479–490

Tubaña BS, Heckman JR (2015) Silicon in soils and plants. Silicon and Plant Diseases. Cham: Springer International Publishin, pp 7–51. https://doi.org/10.1007/978-3-319-22930-0

Waines JG, Ehdaie B (2007) Domestication and crop physiology: roots of green-revolution wheat. Ann Bot 100:991–998

Wang M, Wang R, Mur LAJ, Ruan J, Shen Q, Guo S (2021) Functions of silicon in plant drought stress responses. Hortic Res 8. https://doi.org/10.1038/s41438-021-00681-1

Wasson AP, Richards R, Chatrath R, Misra S, Prasad SS, Rebetzke G, Kirkegaard J, Christopher J, Watt M (2012) Traits and selection strategies to improve root systems and water uptake in water-limited wheat crops. J Exp Bot 63:3485–3498

Wickham H, François R, Henry L, Müller K (2021) dplyr: A Grammar of Data Manipulation. R package version 1.0.5. https://CRAN.R-project.org/package=dplyr

Yin L, Wang S, Liu P, Wang W, Cao D, Deng X, Zhang S (2014) Silicon-mediated changes in polyamine and 1-aminocyclopropane-1-carboxylic acid are involved in silicon-induced drought resistance in Sorghum bicolor L. Plant Physiol Biochem 80:268–277

York LM, Nord E, Lynch J (2013) Integration of root phenes for soil resource acquisition. Front Plant Sci 4:355

Zadoks JC, Chang TT, Konzak CF (1974) A decimal code for the growth stages of cereals. Weed Res 14:415–421